

Radiation resistance and fluorescence of europium doped BGO crystals *

Z.Y. Wei **

World Laboratory, Geneva, Switzerland

R.Y. Zhu and H. Newman

Lauritsen Laboratory, California Institute of Technology, Pasadena, CA 91125, USA

Z.W. Yin

Shanghai Institute of Ceramics, Shanghai, P.R. China

Received 20 July 1990

We report on a study of the radiation resistance and fluorescence of bismuth germanate scintillation crystals doped with europium (BGO:Eu). The transmission spectrum, the light output and the fluorescence spectrum of BGO:Eu crystals were measured before and after irradiation. The radiation resistance of BGO:Eu crystals was found to be increased with increase of europium doping. A red fluorescence emission around 600 nm was found for BGO:Eu samples, which has a 1.5 ms decay time.

1. Introduction

Since the scintillation property of bismuth germanate ($\text{Bi}_4\text{Ge}_3\text{O}_{12}$, i.e. BGO) was discovered [1], the crystal has come to be recognized as an attractive scintillator for applications in medicine, geological exploration, nuclear physics and high energy physics. However, the radiation damage suffered by BGO upon irradiation has limited its use for high precision calorimeters, and thus has received considerable attention [2–7]. Early studies by Kobayashi et al. [2] showed that the degree to which a crystal is damaged is related to the impurity concentration. Work done by Zhou et al. [8,9] revealed that the presence of Cr, Mn, Fe and Pb in BGO leads to substantial radiation softening. In a systematic study carried out at the Shanghai Institute of Ceramics (SIC) it was discovered that europium doping is useful in improving the radiation resistance of BGO crystals, and a new BGO crystal with higher radiation hardness was developed for the L3 experiment at CERN, Geneva [10].

In this report, we present results of a study on radiation resistance and fluorescence of europium doped BGO (BGO:Eu) crystals. Sample BGO crystals with different levels of europium doping were produced at SIC. The scintillation properties and the fluorescence spectra of these crystals before and after irradiation were measured at Caltech. While europium doping enhances the radiation resistance of BGO crystals, it introduces a slow decay fluorescence in the wavelength range of red and a loss of light output. In practice, it is important to choose a proper doping level in producing BGO:Eu crystals with higher radiation resistance.

The next section of this report describes the sample preparation and the experimental instrumentation. Results of our measurements are given in section 3. A discussion and conclusions are presented in section 4.

2. Sample and experiment

2.1. Sample preparation

The Bridgeman–Stockbarger method was used to prepare the BGO crystals. Powders of 5N Bi_2O_3 and 6N GeO_2 were mixed in the stoichiometric ratio of 2:3 to provide a melt. A certain amount of Eu_2O_3 was introduced in the melt during the crystal growth process to

* Work supported in part by U.S. Department of Energy Contracts no. DE-AC03-81-ER40050.

** Permanent address: Shanghai Institute of Ceramics, P.R. China.

Table 1
Doping concentration and dimension of BGO crystals

Crystal	BGO0	BGO1	BGO2	BGO3	BGO4
Dopant	undoped	Eu	Eu	Eu	Eu
Concentration [ppm]	0	5	30	100	1500
Dimension [cm]		2.5×2.5×2.5			1×1×4

produce europium doped crystals. Table 1 lists the europium doping concentration of samples. All samples were polished and annealed at 200°C for 2 h before measurement.

2.2. Irradiation source

The irradiation was performed with a ^{137}Cs γ -ray source at Caltech. The doses were delivered at a rate of about 50 krad/h.

2.3. Light output measurement

The scintillation light yield in units of photoelectron numbers per MeV of energy deposition was measured by using a Hamamatsu photomultiplier (PMT) R2059. The PMT has a bialkali photocathode and a synthetic silica window, which has a spectral response range of 160–650 nm. All BGO samples were wrapped with two layers of teflon tape. The PMT was coupled to the crystals with Dow Corning 200 fluid which has excellent transmittance in the range of 200–820 nm.

The scintillation light collected with a Hamamatsu R2059 PMT was integrated by a LeCroy 3001 QVT multichannel analyzer in the Q mode. A variable integration gate was provided by a LeCroy 2323A programmable dual gate generator. The data taking process was controlled by a μVAXII station through a CAMAC interface. The responses of test samples to a ^{137}Cs γ -ray source were measured, and the peak position of the ^{137}Cs source was subsequently determined by using a Gaussian fit. The peak ADC value was then converted to photoelectron numbers by using calibration curves for each gate width, which were obtained from an LED test run and a subsequent Gaussian fit.

All the measurements were done at room temperature. The systematic error introduced because of the variation of the room temperature was estimated to be less than 2%.

In comparing the light output of BGO before and after irradiation, the crystals were air-coupled to the PMT and the gate width of the multichannel analyzer was fixed at 2 μs . When the crystal was repeatedly removed from the PMT and then reattached to the PMT, the systematic error introduced was found to be less than 1%.

2.4. Transmission spectrum measurement

A Hewlett Packard 8452A diode array spectrophotometer was used for measuring the transmission spectra of samples. This spectrophotometer has a wavelength coverage of 190–820 nm. The data obtained with this spectrophotometer were transferred to a μVAX computer and were analyzed on that computer.

2.5. Fluorescence spectrum measurement

A SLM-4800 spectra fluorometer was used in measuring the emission spectra and the excitation spectra of BGO samples. This spectra fluorometer uses a Xe light source. The wavelength resolution of the instrument can be set between 2 and 8 nm.

2.6. Afterglow measurement

A VSL-337 pulsed nitrogen laser which produces 3 ns wide UV pulses at 337 nm with a repetition rate of 1–20 Hz was used to excite sample crystals. The crystals were coupled to a Hamamatsu PMT R1306 with Dow Corning 200 fluid. The PMT R1306 has a spectral response range covering 300–650 nm. A slow decay light signal was observed with a HP54111D digital scope, and its wavelength was measured to be in the red region (see next section for the details).

In the measurement of the decay constant of this slow decay red light a low-pass filter which passes only light with a wavelength longer than 540 nm was placed between the crystal and the PMT. The data taken were transferred to a μVAXII station.

3. Results

3.1. Scintillation light output

Fig. 1 shows the measured photoelectron yield per MeV as a function of the integration time obtained from a PMT R2059 for four BGO samples before irradiation. The data points with error bars in the figure were fitted to an exponential function:

$$y = S[1 - \exp(-t/\tau)].$$

The numerical results of the fit are also shown in the figure.

All samples have the same time constant of 289 ± 5 ns. The difference of light yield observed has no correlation to the europium doping level in these samples. It is clear that less than 100 ppm europium doping has no effect on either the scintillation light yield or on its decay constant.

After a dose of 2.5 krad from a ^{137}Cs γ -ray source the light yields of these four samples were measured

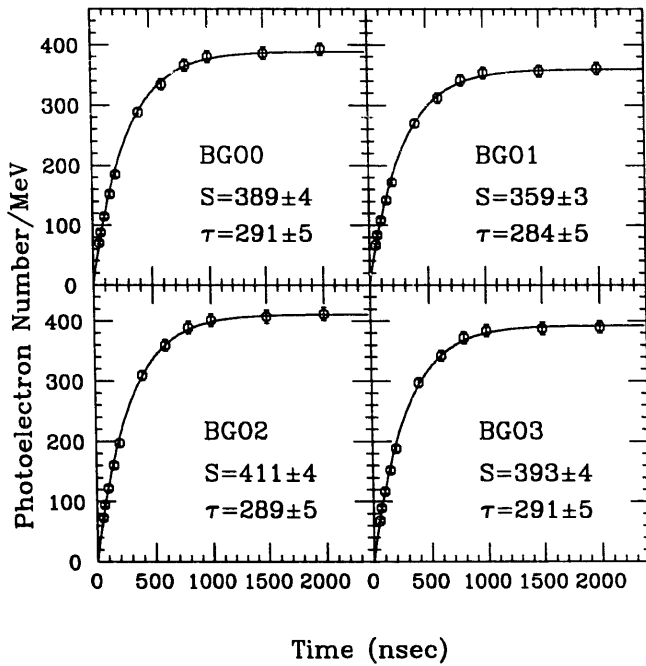


Fig. 1. The light yield of BGO samples.

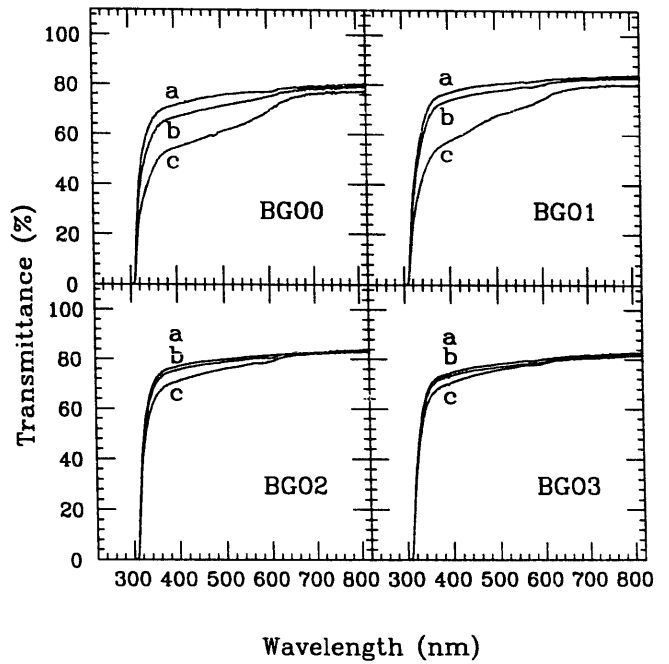


Fig. 3. The transmission spectra of BGO samples before and after irradiation.

again as a function of time. The pulse heights measured ($PH(t)$) were then normalized to the pulse height measured before the irradiation ($PH(0)$) for each sample. Fig. 2 shows the normalized pulse height as a function of the time after the irradiation. The recovery process can be described by a sum of two processes: a fast recovery and a slow one.

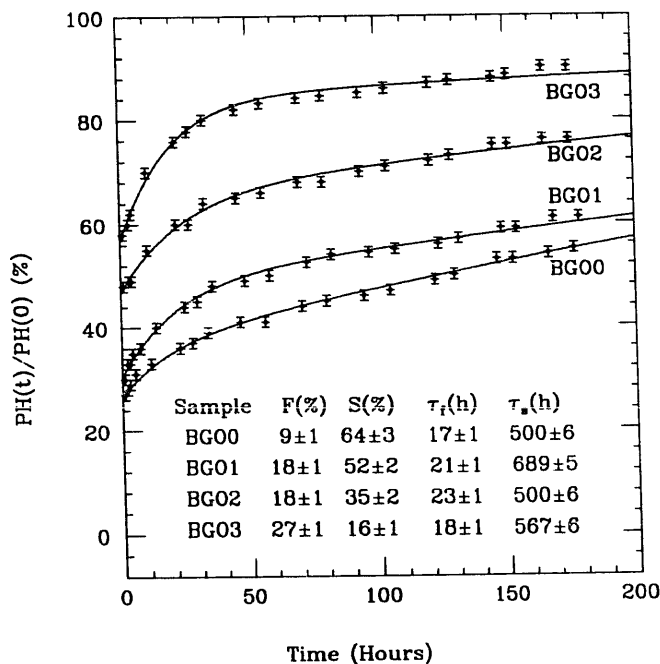


Fig. 2. The light yield of BGO samples normalized to before irradiation.

A fit to the function of $PH(t)/PH(0) = 1 - F \exp(-t/\tau_f) - S \exp(-t/\tau_s)$

gives an excellent description of the recovery. The numerical results of the fit are also listed in fig. 2. For all four samples the fast recovery time, τ_f , is about 20 h, and the slow recovery time, τ_s , is about 500 h. The damage level ($F + S$), especially the slow recovery component (S), decreases with increasing europium doping. This result, therefore, clearly demonstrates the higher radiation resistance of BGO crystals doped with Eu^{3+} . Compared to undoped BGO samples, the europium doped BGO is damaged less and recovers faster.

3.2. Transmission spectrum and radiation induced absorption

The transmission spectra of all samples were measured before and after 2.5 krad irradiation. Fig. 3 shows the transmittance curves obtained before irradiation (a), 15 min after irradiation (c) and 100 h after irradiation (b), respectively, for four samples. It is clear that there is no specific absorption peak introduced by less than 100 ppm europium doping. A transmittance measurement of sample BGO4 which is heavily doped with europium (1500 ppm), however, reveals that specific absorption peaks at 394 and 462 nm are introduced by europium doping. Fig. 4 shows the transmittance of sample BGO4. This and other measurements indicate that a europium doping level beyond 1000 ppm would result in considerable degradation of transmittance and, therefore, light loss.

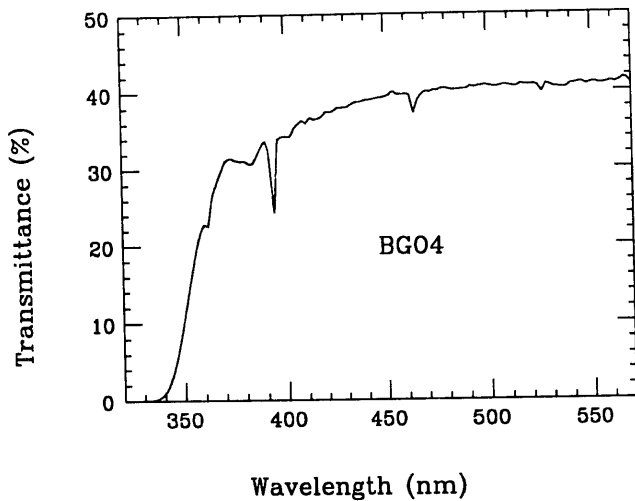


Fig. 4. The transmission spectrum of a heavily doped BGO:Eu sample.

Following our previous work [9] the radiation induced absorption bands were analyzed for these samples. Fig. 5 shows the radiation induced absorption coefficients obtained by analyzing transmittances measured 15 min after the irradiation. It is clear that the radiation induced absorption of europium doped BGO is much less than that of undoped BGO under the same dosage. Each absorption can further be decomposed to three Gaussian bands, and the results of the fit are presented in table 2. These three absorption bands occur at the same energy, regardless of the dopant

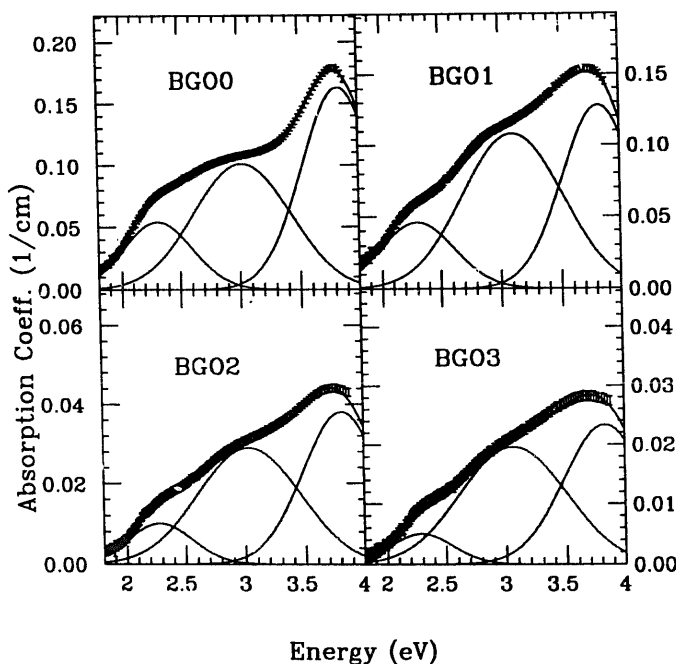


Fig. 5. Gaussian decomposition of radiation induced absorption spectra in BGO.

Table 2
The radiation induced absorption bands in BGO:Eu

Sample	Fitted peak position [eV]		
	E_1	E_2	E_3
BGO0	3.83 ± 0.05	3.02 ± 0.05	2.31 ± 0.05
BGO1	3.82 ± 0.05	3.10 ± 0.05	2.30 ± 0.05
BGO2	3.81 ± 0.05	3.03 ± 0.05	2.28 ± 0.05
BGO3	3.83 ± 0.05	3.06 ± 0.05	2.29 ± 0.05

condition. These bands are the same as what is observed from BGO crystals with different dopant [9].

3.3. Fluorescence spectrum and excitation spectrum

The fluorescence spectra of crystals excited with 309 nm Xe light are shown in fig. 6. All samples show a broad band of blue emission, peaking at 480 nm, which is from the radiative transition of Bi^{3+} : ${}^3\text{P}_1 \rightarrow {}^1\text{S}_0$. In addition to the blue emission, BGO:Eu samples show a weak red emission around 600 nm. The strength of the red fluorescence increases with increasing europium doping concentration. A very strong red emission was observed in the fluorescence spectrum of BGO4 which contains more than 1000 ppm europium. Fig. 7 shows the detailed structure of red emission includes several peaks at 588, 594, 610 and 623 nm, with the maximum at 610 nm.

For the 610 nm component, the excitation spectrum of BGO4 is shown in fig. 8. The corresponding excitation occurs mainly in the wavelength range between 320 and 350 nm. It also occurs at 394 and 462 nm. Fig. 9 shows the fluorescence spectra of europium doped BGO samples when excited with 337 and 462 nm, respectively. We notice that 462 nm is near 480 nm at which the fluorescence of Bi^{3+} reaches its maximum. Part of the scintillation light output of BGO would be absorbed

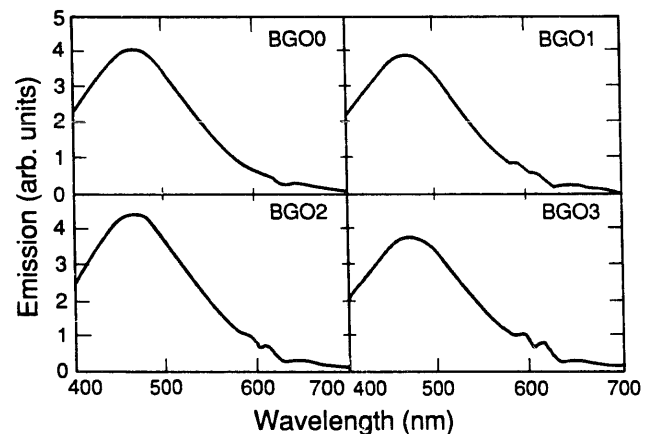


Fig. 6. The fluorescence spectra of BGO excited with 309 nm.

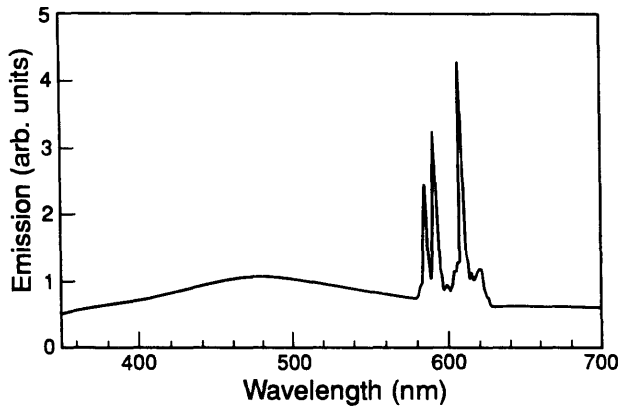


Fig. 7. The fluorescence spectrum of BGO:Eu excited with 309 nm.

by the europium dopant and then produce the emission in the red.

3.4. Afterglow

The fluorescent light pulse of BGO crystals excited with a 337 nm UV laser was observed by an oscilloscope. The BGO sample without doping shows a very clean neat pulse with no afterglow. BGO samples doped with europium show a slow decay component, i.e. afterglow. The amplitude of this slow decay component depends on the doping concentration. The duration of the afterglow is a few ms.

Fig. 10 shows the BGO's fluorescent light pulse obtained with an HP54111D digital scope. By changing the filter the wavelength of the slow component was determined to be longer than 540 nm. The obtained data could be fitted to an exponential function:

$$y = B[\exp(-t/\tau)].$$

The numerical results of the fit are shown in fig. 11, which indicate that the time constant of the afterglow is 1.5 ± 0.1 ms.

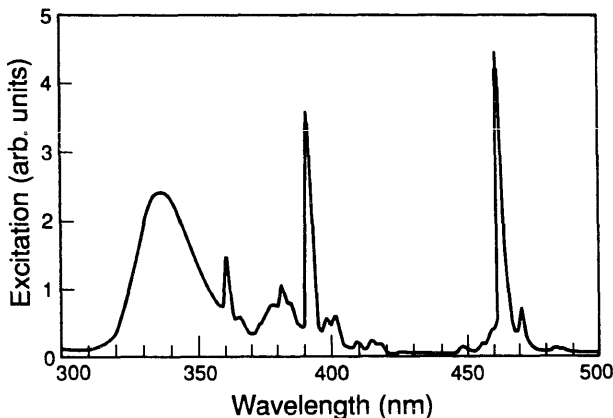


Fig. 8. The excitation spectrum of BGO:Eu for 610 nm emission.

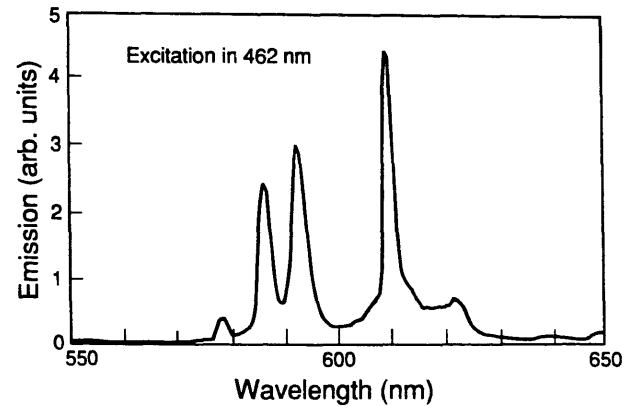
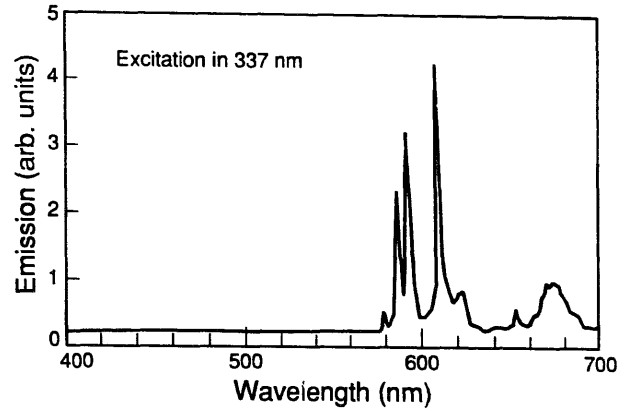


Fig. 9. The fluorescence spectra of BGO:Eu excited with 337 and 462 nm.

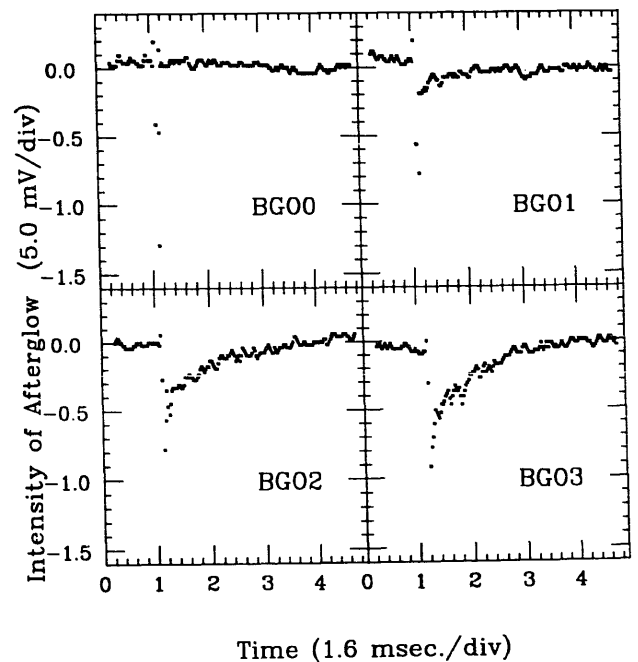


Fig. 10. The BGO light pulse observed with a HP54111D digital scope.

4. Discussion and conclusions

Work done by Zhou et al. [8,9] revealed that three radiation-induced absorption bands occurred at the same energy, 2.3 ± 0.1 , 3.0 ± 0.1 and 3.8 ± 0.1 eV, regardless of the chemical nature of dopant in the BGO crystals. They also concluded that the nature of the color center is not a function of impurity type, but rather of the crystal itself. It was then proposed [11] that oxygen vacancies present in crystals would be the origin of the radiation induced color center. Electrons excited by irradiation are trapped in oxygen vacancies and form the color centers.

According to this model, europium ions Eu^{3+} in a BGO crystal compete with the oxygen vacancies, and trap most of the electrons which are freed in the lattice when the crystal is irradiated. Therefore, the europium doped crystal has a lower color center density under the same irradiation condition.

The emission spectrum of Eu^{3+} ions has been investigated by Raynal et al. [12]. There are several characteristic europium lines corresponding to ${}^5\text{D}_0 \rightarrow {}^7\text{F}_0$ (580 nm), ${}^5\text{D}_0 \rightarrow {}^7\text{F}_1$ (588 and 594 nm), ${}^5\text{D}_0 \rightarrow {}^7\text{F}_2$ (611, 615 and 623 nm) and ${}^5\text{D}_0 \rightarrow {}^7\text{F}_3$ (650, 653, 655 and 657 nm). According to the energy level, the absorption spectrum would show ${}^7\text{F}_0 \rightarrow {}^5\text{D}_1$ (around 525 nm), ${}^7\text{F}_0 \rightarrow {}^5\text{D}_2$ (around 465 nm) and ${}^7\text{F}_0 \rightarrow {}^5\text{D}_3$ (around 395 nm) transitions. Therefore, the observed red emission of BGO:Eu samples has contributions from the radiative transitions ${}^5\text{D}_0 \rightarrow {}^7\text{F}_n$ ($n=0, 1, 2, 3$) of Eu^{3+} . The fluorescence of Eu^{3+} in BGO results from either direct excitation by absorption of the 4f levels themselves, or excitation by absorption of Bi^{3+} ions followed by energy transfer to Eu^{3+} ions.

We summarize our main observations in this report as follows:

- The radiation resistance of BGO crystal is improved by europium doping. Compared with normal BGO, the BGO:Eu has less radiation damage and a faster recovery process.
- The fluorescence of BGO:Eu contains a broad blue emission and a red emission. The blue emission originates from the Bi^{3+} transition ${}^3\text{P}_1 \rightarrow {}^1\text{S}_0$, which has a time constant of 290 ± 5 ns. The red emission was caused by the radiative transitions of ${}^5\text{D}_0 \rightarrow {}^7\text{F}_n$ ($n=0, 1, 2, 3$) of Eu^{3+} , which has a slow time constant, around 1.5 ms, and forms the afterglow.

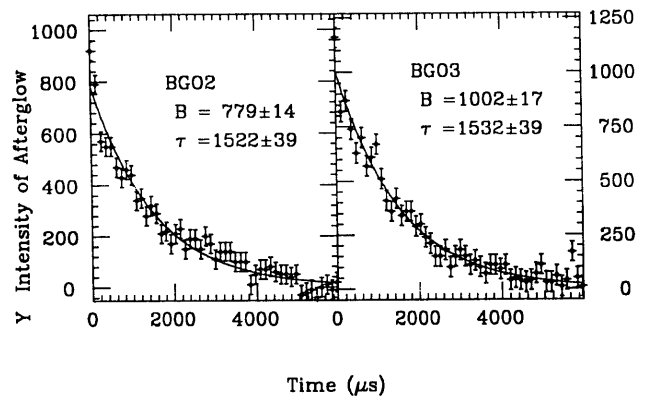


Fig. 11. The decay time of the afterglow of BGO:Eu.

- The fluorescence of Eu^{3+} in BGO results from either direct excitation by absorption of the 4f levels themselves, or excitation by absorption of Bi^{3+} ions followed by energy transfer to Eu^{3+} ions. This explains that a higher doping would result in a light yield decrease of BGO.

Acknowledgements

The authors would like to thank Mr. M. Youngquist of Caltech for the use of the SLM-4800 Spectra Fluorometer. Mr. L. Wei and Mr. Y. Mao helped in the on-line readout of the HP54111D digital scope.

References

- [1] M.J. Webber and R.R. Monchamp, *J Appl. Phys.* 44 (1973) 5496.
- [2] M. Kobayashi et al., *Nucl. Instr. and Meth.* 206 (1983) 107.
- [3] S. Wen and C. He, *Nucl. Instr. and Meth.* 219 (1983) 333.
- [4] M. Cavalli-Sforza, *Proc. Int. Workshop on Bismuth Germanate* (Physics Department Report, Princeton University, 1982).
- [5] C. Laviron and P. Lecoq, *Nucl. Instr. and Meth.* 227 (1984) 45.
- [6] Ch. Bieler et al., *Nucl. Instr. and Meth.* A234 (1985) 435.
- [7] G.J. Bobbink et al., *Nucl. Instr. and Meth.* 227 (1984) 470.
- [8] T.Q. Zhou, *Master Thesis* (1986).
- [9] R.Y. Zhu et al., *Caltech preprint CALT-68-1392* (1985).
- [10] Z.W. Yin et al., *Nucl. Instr. and Meth.* A275 (1989) 273.
- [11] Z.Y. Wei et al., *Ren Gong Jing Ti* 17 (1988).
- [12] F. Raynal et al., *Mater. Res. Bull.* 11 (1976) 731.